

A 9-element Tapered slot Antenna Array fed with T-Junction Power Divider for X-band Radar Applications

Babu Saraswathi K. Lekshmi* and I. Jacob Raglend**

Abstract : In this paper, a nine-element dual layered exponentially tapered slot antenna (TSA) is presented. The array is composed of 1:9 T-junction power divider which acts as a feed network with uniform distribution and 1x9 TSA element array. The array elements are designed to have a compact size with maximum reflection coefficient less than -10 dB over the X-band operating frequency. The simulated results show good agreement with the measured results for the fabricated antenna array. Measured results of single element and a center element excited in array environment, both have a wide 3-dB beam width greater than 107° in the principal planes, which is capable of a linear array with wide scan angle $\pm 60^\circ$. The measured array has a 3-dB beamwidth of 11 degrees with side-lobe level of -12dB at 10GHz with a gain of 12dBi. These characteristics make the antenna array suitable for X-band airborne radar applications.

Keywords : Vivaldi antenna, strip line feed, wideband, wide beam, slot line, Radar, VSWR, tapered slot antenna.

1. INTRODUCTION

The tapered slot antenna (TSA) was presented by Lewis *et al.* in 1974 [1]. Its potential for wideband and wide-scan arrays makes it a main candidate for high performance phased array antenna. Vivaldi antenna is a type of TSA used in an Ultra wide band (UWB) technology. It was introduced by Gibson [2, 3] in 1979, has an exponentially tapered slot line. It provides wide bandwidth, low cross polarization and directive propagation at microwave frequencies. Vivaldi antennas are low cost, easy to fabricate and fairly insensitive to dimensional tolerances in fabrication process due to the printed circuit technology used in the construction of these antennas [4]. Moreover, Vivaldi arrays, which are small in size, simple and weightless, enable compact arrays and they are highly efficient [5].

Phased arrays are necessary to operate over wide bandwidths and wide scan angle to provide multifunction operation in both telecommunication and radar systems [6,7]. The multi-function wideband arrays which is capable of simultaneous and time interleaving, electronic warfare and communications functions [10]. In response to that need, one compact TSA design for airborne radar applications has been proposed in this paper. The TSA with Strip line feed network, which can operate over the X-band frequency and scan angle greater than $\pm 60^\circ$ in H-plane and E-plane. The complete design and optimization of the antenna has been reproduced using an electromagnetic simulator, ANSYS High Frequency Structure Simulator (HFSS) [9]. The opposite side of the substrate includes a micro strip feed and a crossover transition that excites a rectangular cavity on the slot side. The energy from this cavity is transferred to the slot line taper. This work mainly focuses on the design of the slot taper so as to maximize power

* Babu Saraswathi K. Lekshmi, Noorul Islam University, Kumaracoil, Kanyakumari, India, 629180, E-mail: kavitha20012@gmail.com

** Jacob Raglend. I, Professor, VIT University, Vellore, India, 6320140. E-mail: jacobraglend@rediffmail.com

transformation and minimize reflection. For exponential tapers, a close form equation has been applied for taper design in order to determine the exponential opening rate [8].

Several studies about the X-band phased array antenna for wide-scan applications have been recently proposed [13, 14]. The Bengt *et al.* [13] developed a slotted waveguide antenna with achieving scan area less than $\pm 40^\circ$ in X-band. Chen and Wang [14] developed an array with feed network integrated into the structure of the antennas. But the measurement results were not mentioned in their work to validate the performance of the array. When designing antenna array, problems associated with the integration of antenna element and feeding network such as mutual coupling between antenna elements must be addressed.

In this paper, a nine-element linear X-band antenna array has been designed and the characteristics of the proposed array are investigated numerically and validated experimentally. The outline of this paper is as follows. In Section 2, the geometry of the proposed antenna is presented. This compact antenna element is used to compose the X-band antenna array. In Section 3, the design of the array with uniform distribution is presented to analyze the element in an array environment. In Section 4, the design of T-junction power divider which is used as a feed network for this array is described. Measured results are presented in Section 4 and the conclusions are summarized in Section 5.

2. TAPERED SLOT ANTENNA ELEMENT DESIGN

Parametric Study

Strip line-fed Vivaldi antennas are comprised of a Strip line-to-slot line transition, a Strip line stub, a slot line cavity and a tapered slot. Figure 1 illustrates the geometry of the Dual layered tapered slot antenna assembly and the details of the various parts involved in the design. The model depicts two substrates, aligned back to back, consisting of radiating flare geometries on the two opposite faces. One of the substrates is etched completely on the opposite side of the flare and the other substrate consists of strip line feed being printed and sandwiched between the two substrates containing the flares.

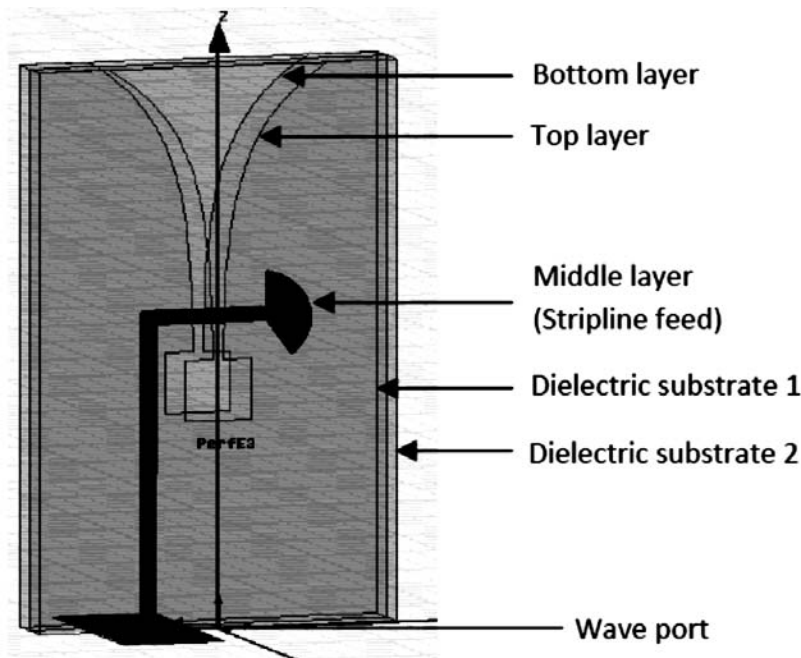


Figure 1: Schematic of Vivaldi Tapered slot antenna geometry

The Figure 2 shows the exploded view of layers forming the complete antenna assembly viz., bottom layer, top layer and the middle layer (strip line feed). The parametric study and design of the single element Vivaldi antenna consists of three models: 1. Strip line model, 2. Strip line & Slot line model, and 3. Antenna model.

A Strip line model is formed to match the characteristic impedance of the Strip line to that of the transmission line (feeding the antenna) and the slot line. A substrate material with dielectric constant, greater than that of the air shall be used in order to get constant antenna impedance and realize impedance matching. Dielectric constant and substrate thickness are the parameters determining the performance and radiation pattern, *ie.*, the beam width, side lobe level and the gain of the antenna. The Slot line width, which is also known as throat width, is the separation between the Slot line conductors which is before the tapered section. Throat width, an important parameter to be optimized, is to be determined carefully in order to get the desired return loss. Strip line to slot line transition defines the operational bandwidth and the slot line width is a main parameter of this structure. Any change (increase/decrease) from the optimized value of the slot width degrades return loss response drastically lowering the effectiveness of the strip line to slot line transition. Antenna length should be greater than a free space wavelength at the lowest frequency of operation, 8GHz in this case, increasing the antenna length provides a wider bandwidth. Finally, the antenna model is constructed specifying the uniform slot line length, taper length and rate, mouth opening and the edge offset.

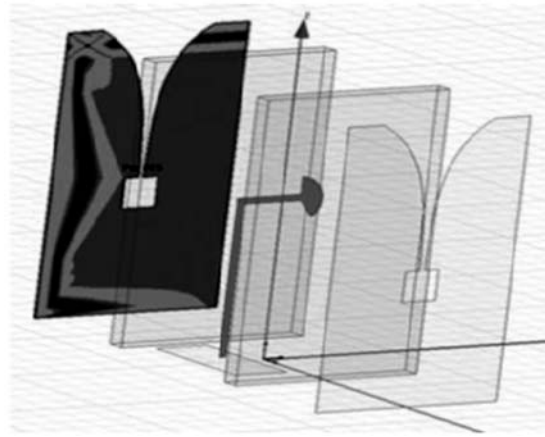


Figure 2: Exploded view of tapered slot antenna assembly

The design parameters of a Dual layered exponentially tapered slot antenna with square cavity and radial stub strip line feed are given in Figure 3. The RT Duroid5880 dielectric substrate is used for this design with relative permittivity $\epsilon_r = 2.2$ and thickness $t = 0.7$ mm. The strip line/slot line transition is specified W_{ST} (strip line width) and W_{SL} (slot line width). The exponential taper profile is defined by the opening rate R and two points $P_1(z_1, y_1)$ and $P_2(z_2, y_2)$

$$y = c_1 e^{Rz} + c_2 \quad (1)$$

Where,

$$c_1 = \frac{y_2 - y_1}{e^{Rz_2} e^{Rz_1}}$$

$$c_2 = \frac{y_1 e^{Rz_2} - y_2 e^{Rz_1}}{e^{Rz_2} e^{Rz_1}}$$

The taper length L is $z_2 - z_1$ and the aperture height H is $2(y_2 - y_1) + W_{SL}$. In the limiting case, where opening rate R approaches zero, the exponential taper results in a so-called linearly tapered slot antenna (LTSA) for which the taper slope is constant and given by $s_0 = (y_2 - y_1)/(z_2 - z_1)$. For the exponential taper defined by equation (1), the taper slope s changes continuously from s_1 to s_2 , where s_1 and s_2 are the taper slope at $z = z_1$ and $z = z_2$, respectively, and $s_1 < s < s_2$ for $R > 0$. The taper flare angle is defined by $\alpha = \tan^{-1}s$. The flare angles, however, are interrelated with other defined parameters, *ie.* H , L , R and W_{SL} .

The Table 1 depicts the dimensions of Vivaldi antenna. The bandwidth of the antenna is improved with these non-uniform stubs and also noted that radial stub is more advantageous regarding the overlapping between strip line and slot line stubs. The strip line feeding increases the antenna bandwidth compared with the micro strip feeding.

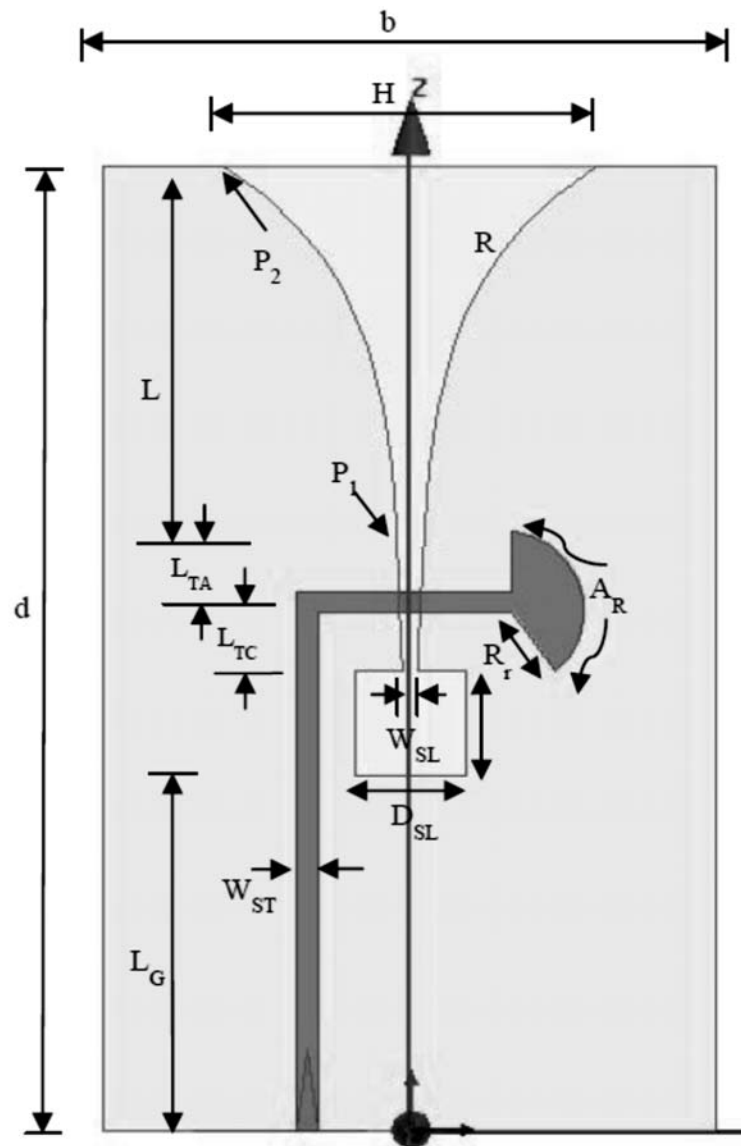


Figure 3: Definition of parameters of Vivaldi Tapered slot antenna

2.2. Simulations

The simulation results are obtained using ANSYS Electromagnetic simulator HFSS. The S-parameter plots in Figure 4 shows the $\text{dB}(S(1,1))$ parameter, which is less than -10dB for an isolated element over the frequency of 8 GHz to 12 GHz. The simulated radiation patterns of an isolated Vivaldi antenna element illustrate the achieved 3-dB beam width (or) half power beam width (HPBW) greater than 120° in the two principal planes and a gain of approximately 4 dBi as shown in Figure 5. From the radiation pattern, it can be inferred that for the Azimuth cut ($\Phi = 0^\circ$), the scan angle is $\pm 68^\circ$ and 3-dB beam width is 136° . Further, in the Elevation cut ($\Phi = 90^\circ$), the scan angle is $\pm 60^\circ$ and 3-dB beam width is 120° . It is observed that low cross polarization has been achieved for an isolated single element as shown in Figure 11.

2.3. Fabrication

The Vivaldi Tapered Slot antenna is fabricated with optimized dimensions depicted in Table 1. The antenna is fabricated with RT/duroid5880 substrate with the permittivity $\epsilon_r = 2.2$ and thickness 0.7mm. The antenna has two substrates, a top and a bottom, consisting of radiating flare geometries on the two opposite faces. One of the substrates is etched completely on the opposite side of the flare and the other substrate consists of strip line feed, printed and sandwiched between the two substrates containing the flares. The top, bottom

and middle layers form the complete antenna. It is fabricated using printed circuit processing techniques. The two substrates are bonded using Araldite adhesive substance without any air gaps. The center pin of the connector is soldered to the Stripline and the outer pins of the connector is soldered to the slotline ground planes in order to realize the ground connection of the feeding. The photograph of the fabricated Vivaldi antenna is shown in Figure 6.

The isolated single element is simulated with the stripline configuration which is TEM mode, but the fabricated model is hard to connect the connector because of stripline geometry. So the transition has been made from stripline to microstrip line configuration to connect RF Connector. A V-shaped cut has been introduced above the stripline to connect the SMA connector. As we know that microstrip is the Quasi TEM mode, optimization has been made to match with 50Ω connector and the strip line. The final simulated model is shown in Figure 3.

Table 1
Dimensions of Vivaldi Antenna

<i>Parameters</i>	<i>Specifications (in mm)</i>
Strip line width (W_{ST})	0.5
Angle of radial strip line stub (A_R)	130°
Antenna width (b)	14.2
Antenna length (d)	24.1
Length of slot line cavity from ground plane (L_G)	8.9
Aperture height (H)	8.5
Taper Length (L)	10.6
Opening Rate (R)	0.36
Slot width (W_{SL})	0.2
square slot line cavity (D_{SL})	2.6x2.6
Radius of radial strip line stub (R_r)	2.02
Distance from the transition to the taper (L_{TA})	1
Distance from the transition to the slot line cavity (L_{TC})	1

The measured results of $dBS(1,1)$ parameter and Radiation patterns are shown in Figures 8(a) and 9. The measured result of S-parameter is compared with simulated results shown in Figure 4. Due to some manufacturing tolerances while bonding the two substrates together, leads to the difference in the simulated and actual overall thickness of the substrate.

2.4. Measurements

The S-Parameter of fabricated antenna is measured using a Vector Network Analyzer and the radiation patterns are observed in Anechoic Chamber. The measured S-parameter of a single element is less than -10dB over the band of frequency from 8.9 GHz to 10.4 GHz with the resonating center frequency of 9.5GHz as shown in Figure 8. The Figure 9 shows the measured radiation patterns in H- and E-planes, respectively, of an isolated single element illustrating the achieved 3dB beam width greater than 101.32° in the H- and E-planes with a gain of 4 dBi at X-band operating frequency.F

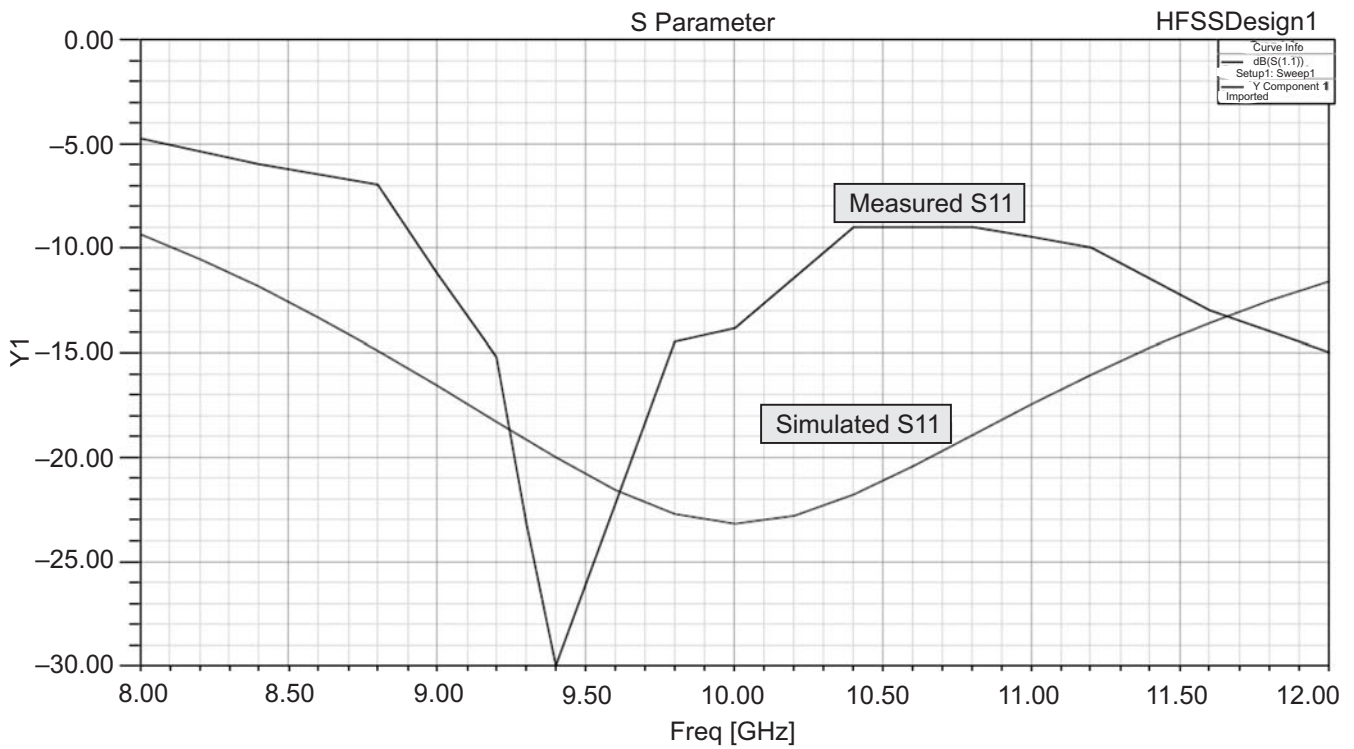


Figure 4: Measured and Simulated S-parameter results of Vivaldi antenna

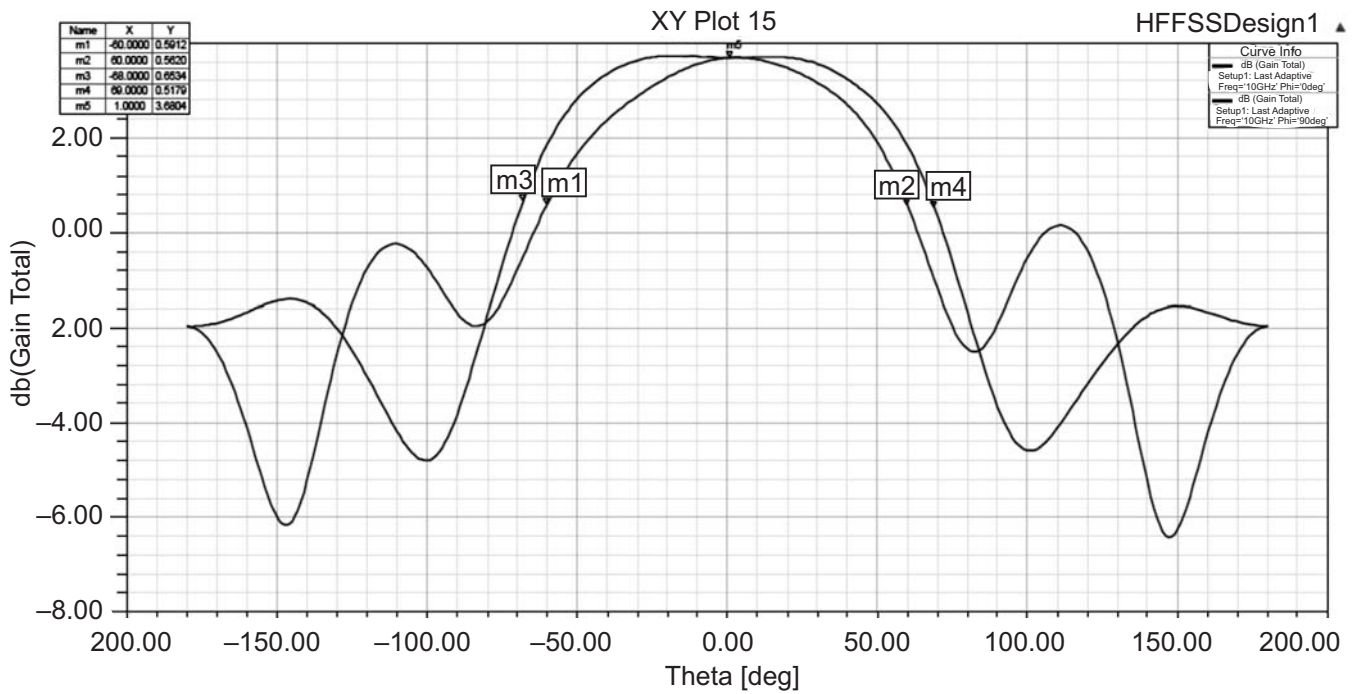


Figure 5: Simulated radiation patterns of Vivaldi antenna at 10GHz in E- and H-planes

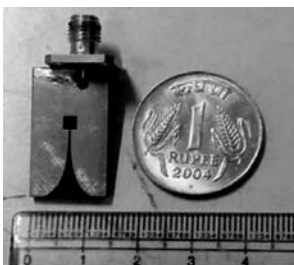


Figure 6: Fabricated Vivaldi antenna

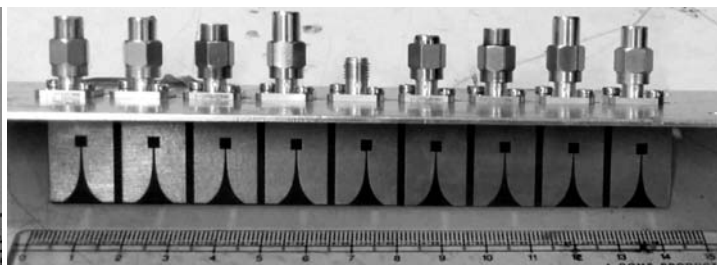
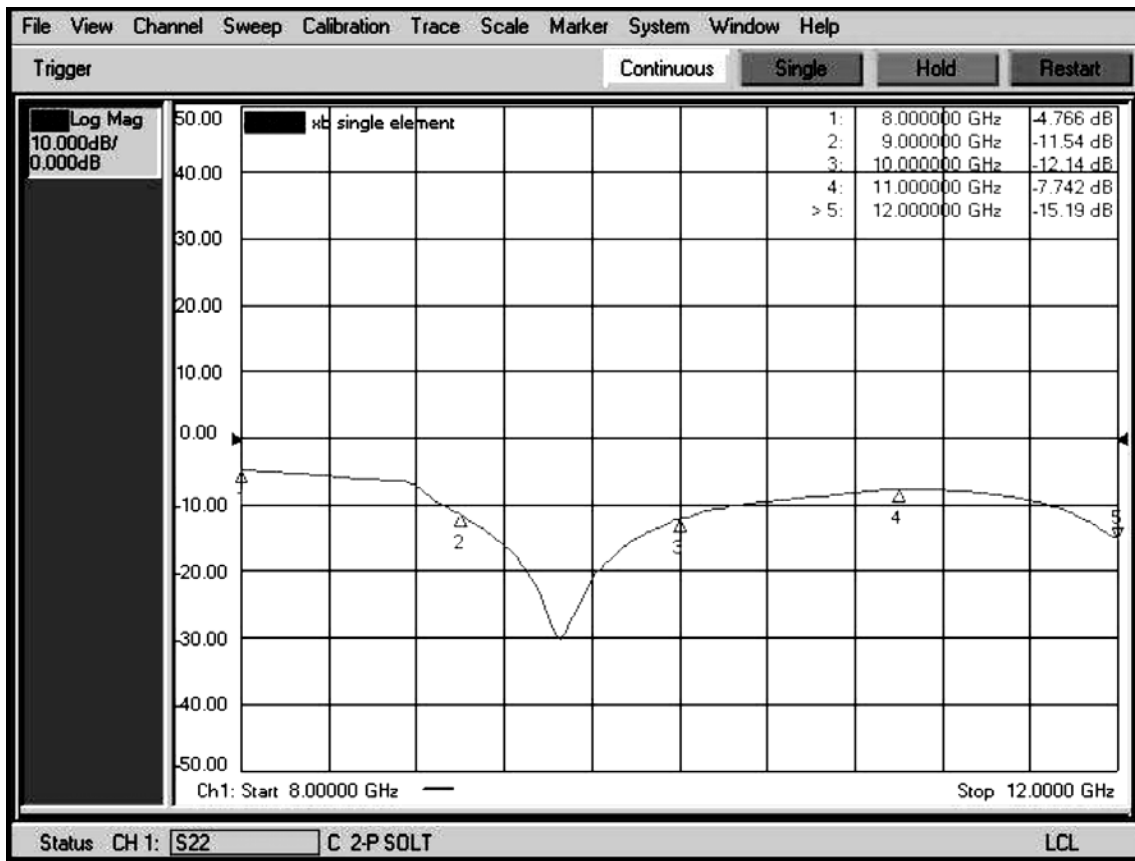
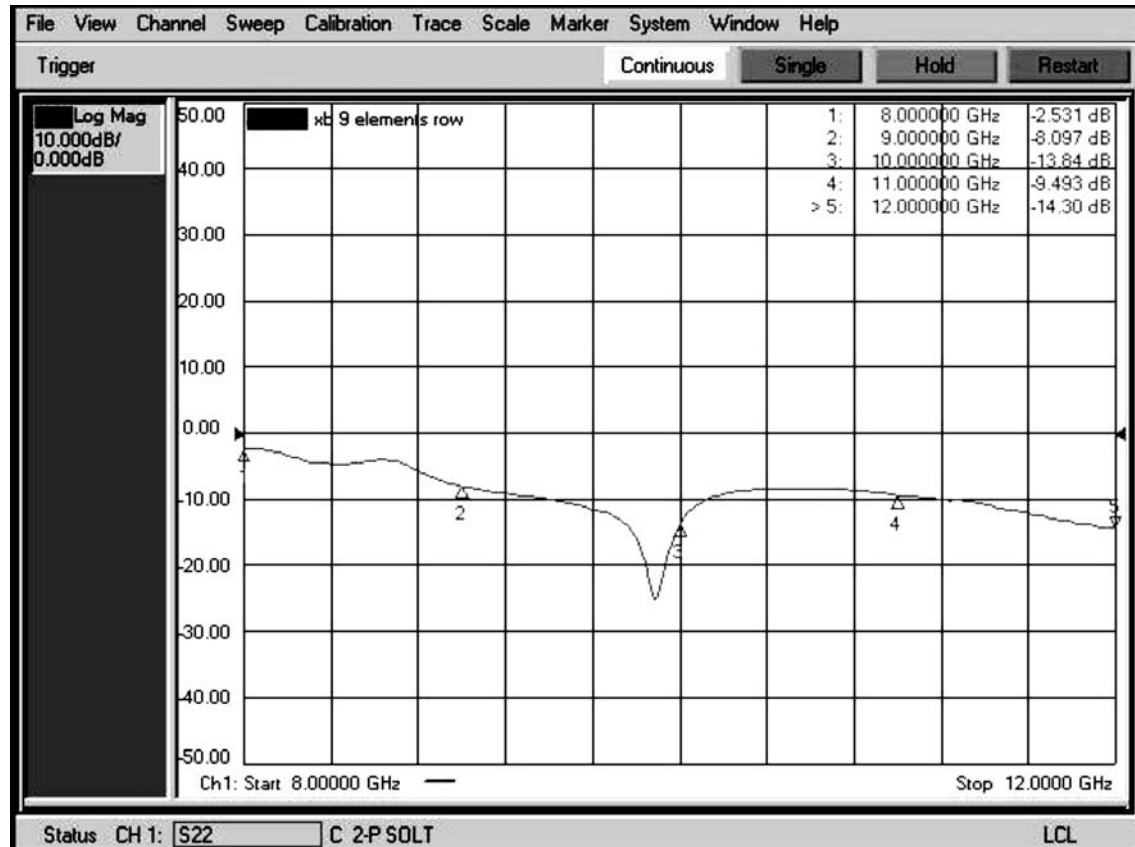


Figure 7: Fabricated Vivaldi antenna linear array

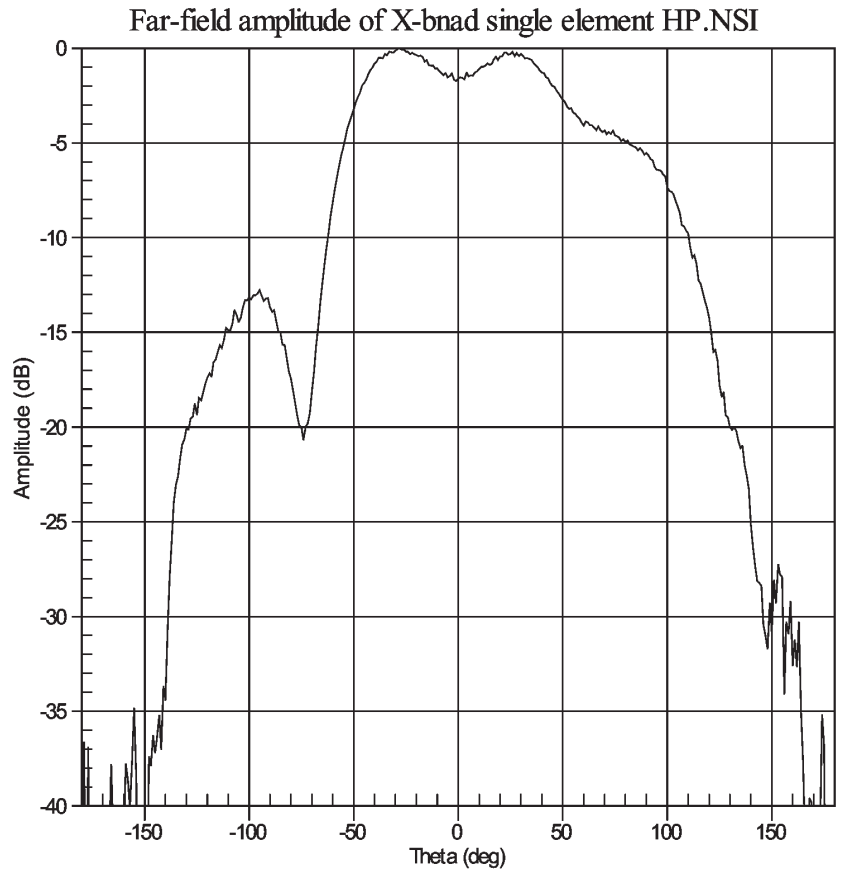


(a)

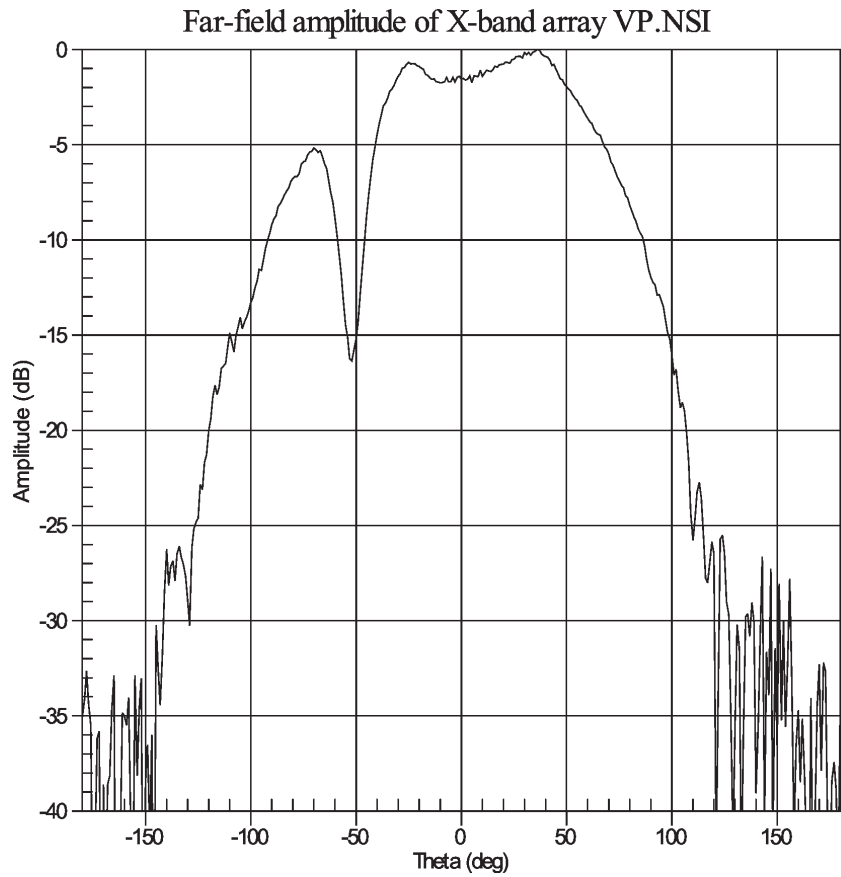


(b)

Figure 8: Measured S-parameter performance of TSA (a) isolated environment and (b) array environment

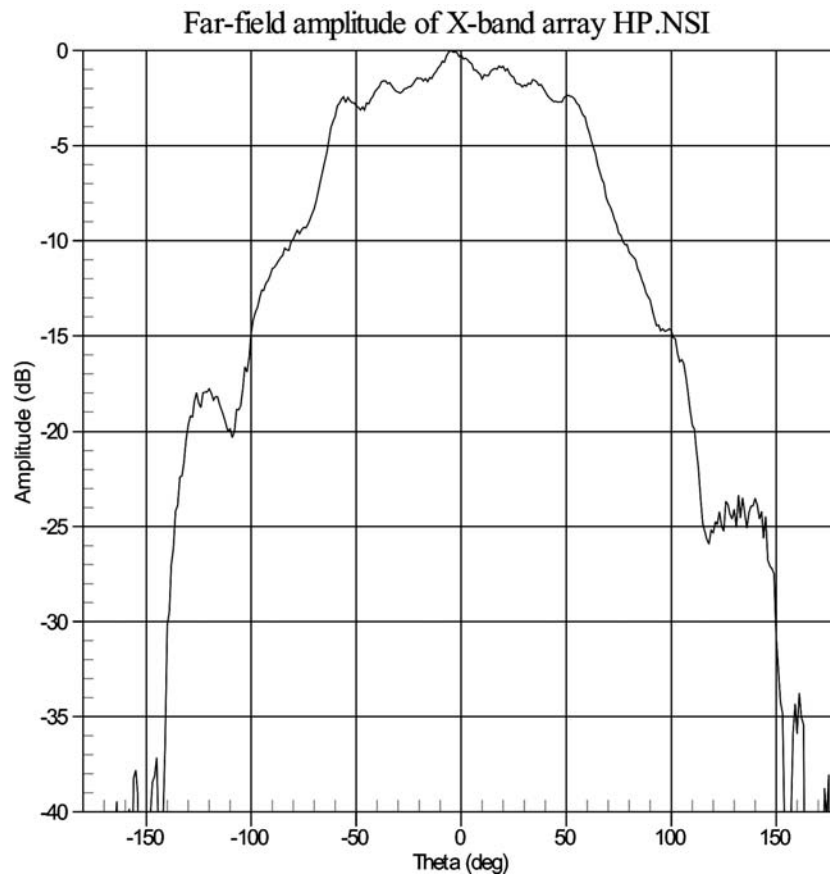


(a) H-plane

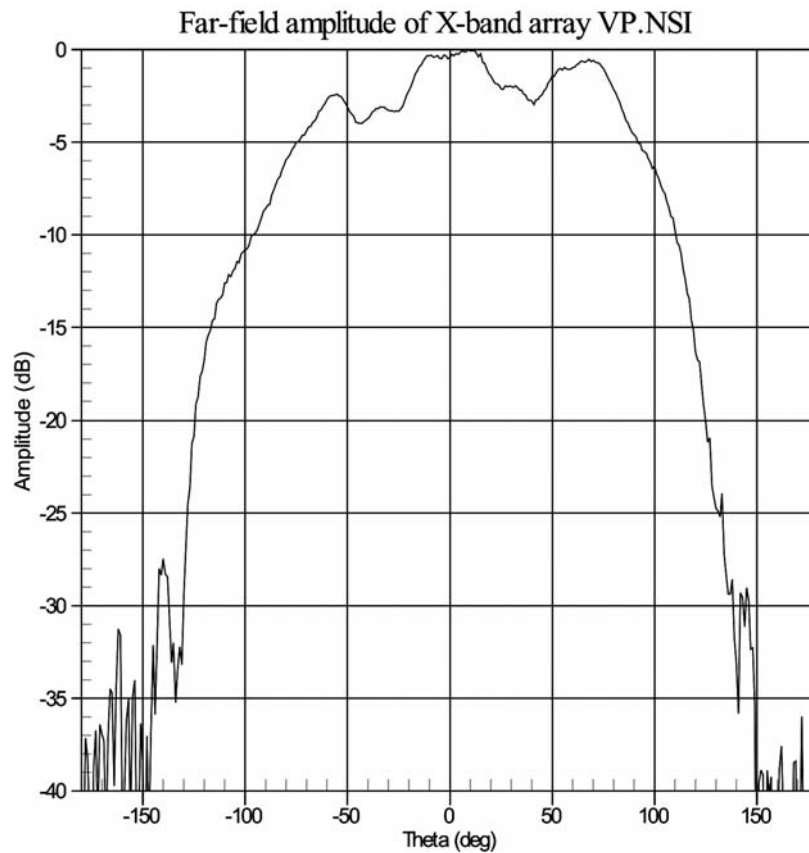


(b) E-plane

Figure 9: Measured Radiation patterns of isolated Single element at 10GHz



(a) H-plane



(b) E-plane

Figure 10: Measured Radiation patterns of a center element in array environment at 9 GHz

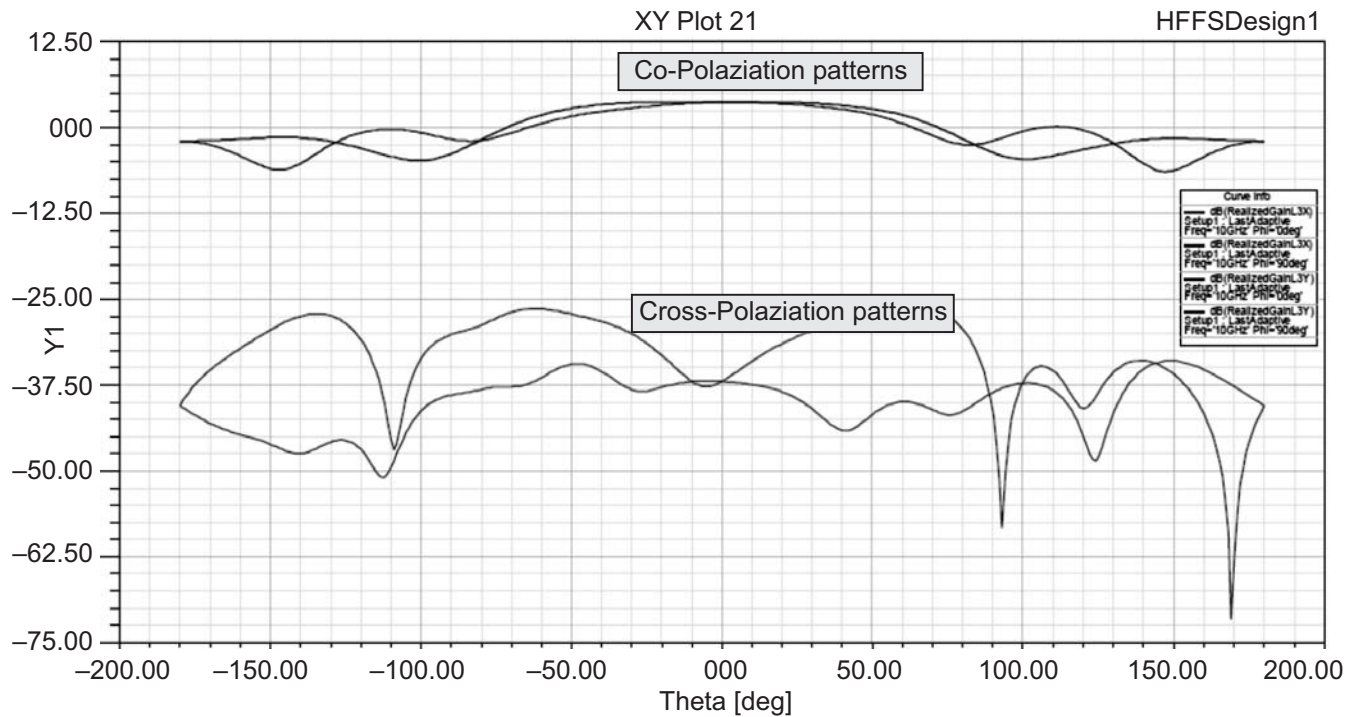


Figure 11: The simulated Co-polarization and Cross-polarization patterns of isolated single element

3. TAPERED SLOT ANTENNA ARRAY DESIGN

The Array performance strongly depends on the mutual coupling both in the wide bandwidth and the wide scanning arrays. The linear array is designed with 9-elements, displaced a distance, dy . All the coupling effects are accounted in the scan element pattern. The Scan element pattern (SEP) is obtained by exciting only one of the elements, the other elements are terminated with matching loads [11]. The Figure 7 shows the fabricated one-dimensional Vivaldi antenna array. To derive a desired specification, an array of 9-elements have been arranged in a linear grid with a spacing, $dy = 16\text{mm}$. The inter-element spacing is defined by the Equation (2).

$$dy = \frac{\lambda}{1 + \sin\theta} \quad (2)$$

Where λ is the wavelength. Therefore, the physical element spacing is restricted by the minimum operating wavelength (highest frequency) and maximum scan angle. When the antenna is in array environment, S_{11} is the impedance matching parameter for an antenna element. The principal performance parameter of a wideband array is the active reflection coefficient. That is the percentage of power reflected back from the radiating element, when all the elements in an array are fully excited. The active reflection coefficient can be calculated by the following function

$$\Gamma_m(\theta) = \sum_{n=1}^N S_{mn} e^{-iknd \sin\theta} \quad (3)$$

When $k = (2\pi/\lambda)$, m is the m^{th} element and S_{mn} is the S parameter between the m^{th} element and n^{th} element. In this function, the mutual coupling between the elements S_{mn} are taken into account. The center element is excited in array environment and the other elements are connected with 50Ω matched loads.

3.1. Measurements

The RF connectors used for feeding the antenna elements are SMA series connectors. After terminating all the elements with the matched loads, except the center element, *ie.*, 5th element in the linear array (in Figure 7), the return loss and the principal plane pattern measurements were carried out for analyzing the effects of embedded element performance. The measured active S-parameter of the center element, *ie.*, 5th

element which is less than -10dB over the desired frequency band, is achieved as shown in Figure 8 (b). The measured mutual coupling is -16 dB for the immediate neighboring element of the center element.

The measured radiation patterns of the center element at the center frequency, along with all other elements in linear array being terminated has been shown in H- and E-planes respectively in Figures 10 (a & b). It is observed that HPBW of 104° and 107° in H- and E- planes, respectively, has been achieved. Some reduction in HPBW and the increase in cross-polarization have been observed due to the coupling from neighboring array elements and the presence of a metallic ground plane on which Vivaldi antenna is mounted for pattern measurement.

3.2. Simulations

The simulated radiation patterns of uniformly distributed 9-elements linear array is shown in Figures 17 illustrates the results of HPBW of 11° in E-plane ($\Phi = 90^\circ$) and 130° in H-plane ($\Phi = 0^\circ$). The good radiation characteristics are obtained with a gain of 13 dBi, with low Side lobe level (SLL) is -13dB down from the main lobe.

The Figure 19(a & b) shows the simulated results of scanned beam patterns at 10GHz at different beam steering angle ($\approx Nkd \sin \theta$) $\pm 15^\circ$, $\pm 30^\circ$, $\pm 45^\circ$ and $\pm 60^\circ$ of uniformly illuminated 9-elements antenna array including the element pattern showing the ability of array can scan over the desired scan volume around 120° . These studies shows the ability of designed widebeam Vivaldi antenna is the suitable element for wide angle scanning phased array antenna operating at X-band frequency.

Planar Array performance Results

A planar array of $9 \times 9 = 81$ elements with the rectangular grid arrangement having inter-element spacing (in Figure 18), from equation (2) in X- and Y- direction is calculated as $dy = 16\text{mm}$ and $dx = 15.56\text{ mm}$. The radiation patterns obtained in E- and H-planes are shown in Figures 18 with the gain of 23dBi, the HPBW is 11° in E- and H-planes with SLL of -13dB down from the main lobe.

4. T-JUNCTION POWER DIVIDER DESIGN

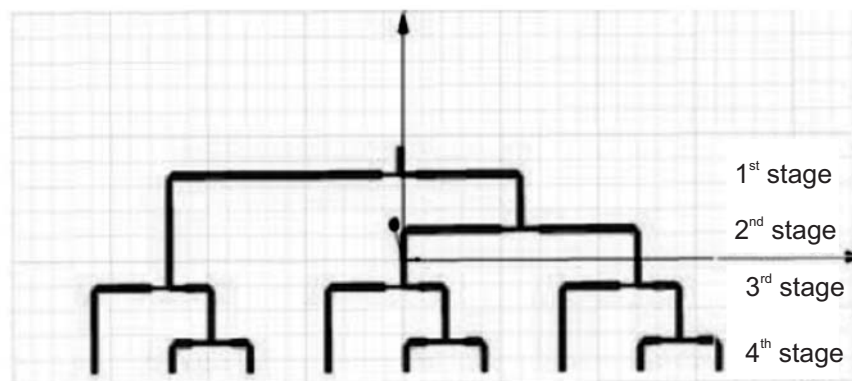


Figure 12: Design of uniformly distributed 1:9 way equal T-junction power divider

A wideband T-junction power divider is required to feed the TSA array shown in Figure 12. The T-junction power divider has 4-section, which provides signals with balanced amplitudes and phases from the output ports, is designed to compose the 9-way feed network for the Tapered slot antenna array. The 4-stage T-junction corporate power divider makes use of an unequal split T-junction power divider in the 1st stage. The 2nd and 3rd stages are composed of unequal T-junction power splitters to achieve the required power distribution. The Spacing between Junctions is equally spaced at 0.54λ . The fabricated 1:9 T-junction power divider for the TSA with uniform distribution operating at 9-10GHz frequency is shown in Figure 14. The input and the nine output ports are matched at a characteristic impedance of 50Ω so that the power divider can be directly connected with the tapered

slot antennas. The nine phase matched RF cables are used to connect the Vivaldi antenna elements with the output ports of 1:9 way power divider circuit.

4.1. Fabrication

The Figure 13 shows the geometry of the tapered slot antenna array. This structure is composed of 9 identical radiating elements and connected by a feeding network. This power divider is built by using microstrip transmission lines on FR4 substrate board with dielectric constant $\epsilon_r = 4.4$ and substrate thickness of 1.6 mm.

4.2. Measurements

The return loss and VSWR are measured using VNA and the measurement setup is shown in Figure 13. The radiation patterns are measured in the anechoic chamber shown in Figure 14. The S-parameter results are obtained less than -10dB over the frequency 8-11GHz as given in Figure 15. The radiation patterns with 3-dB beam width of 12° and the side lobe level lower than -12dB are measured at 9GHz and at 10GHz operating frequency are shown in Figures 16.

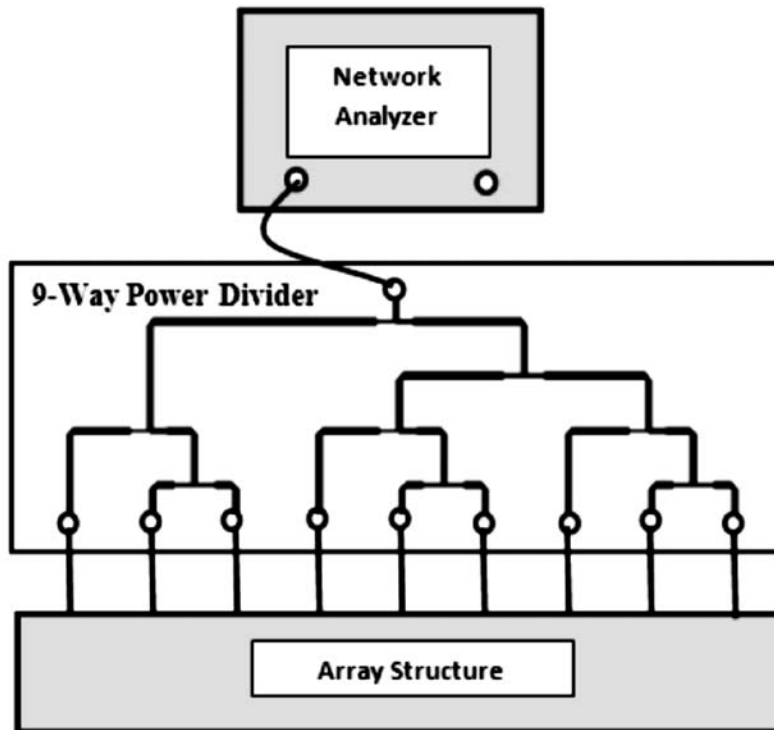


Figure 13: Array Return loss measurement setup

4.3. Performance Comparisons

The designed Vivaldi antenna has been optimized in the infinite array environment. The unit cell approach is simulated to optimize the antenna element in the infinite array environment for rectangular lattice arrangements [12].

The Table 2 shows the performance comparisons between isolated single element and a center element excited in an array environment. It is observed that the simulated and measured results are in good agreement. The gain is observed around 4dBi, low cross polarization and maximum beam width around 107° over the desired X-band frequency. The ripples in radiation patterns can be reduced by covering the ground plane with some absorbing materials. These studies demonstrates the suitability of the designed Vivaldi antenna as a better choice for active phased array operating at X-band for airborne radar applications.

Table 2
Performance Comparisons of Vivaldi Antenna

Antenna Parameters	Simulated results of Vivaldi antenna in Isolated environment	Measured results of Vivaldi antenna in Isolated environment	Measured results of a center element in Array environment
Resonant Frequency(GHz)	10	9.5	9.8
dB(S(1,1)) at center frequency (dB)	-23	-30	-26
Gain(dBi)	4	4	4
Bandwidth(GHz)	8 – 12	8.9 – 10.4	8 – 11
3-dB Beam width at H-plane	130°	101°	104°
3-dB Beam width at E-plane	120°	101°	107°

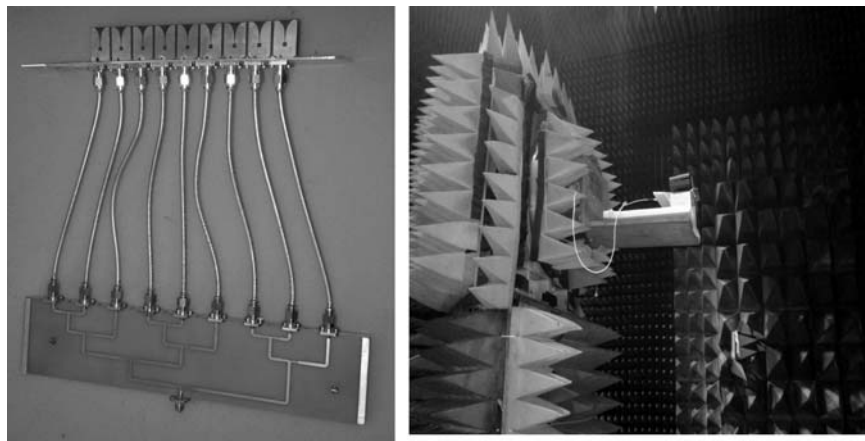
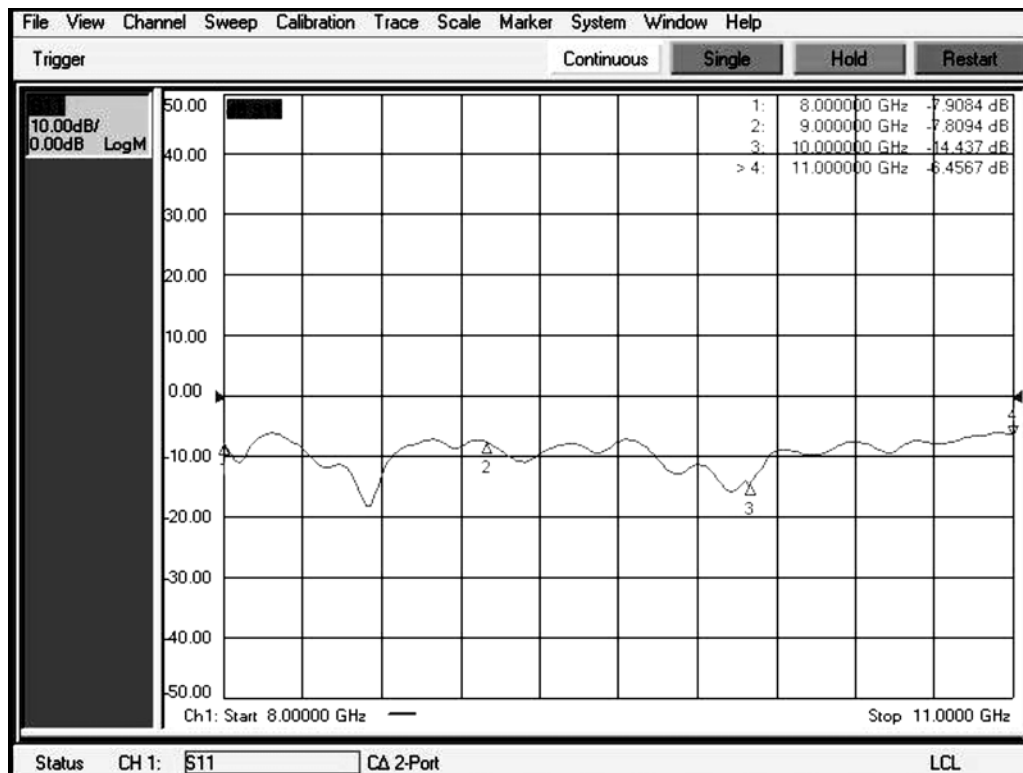
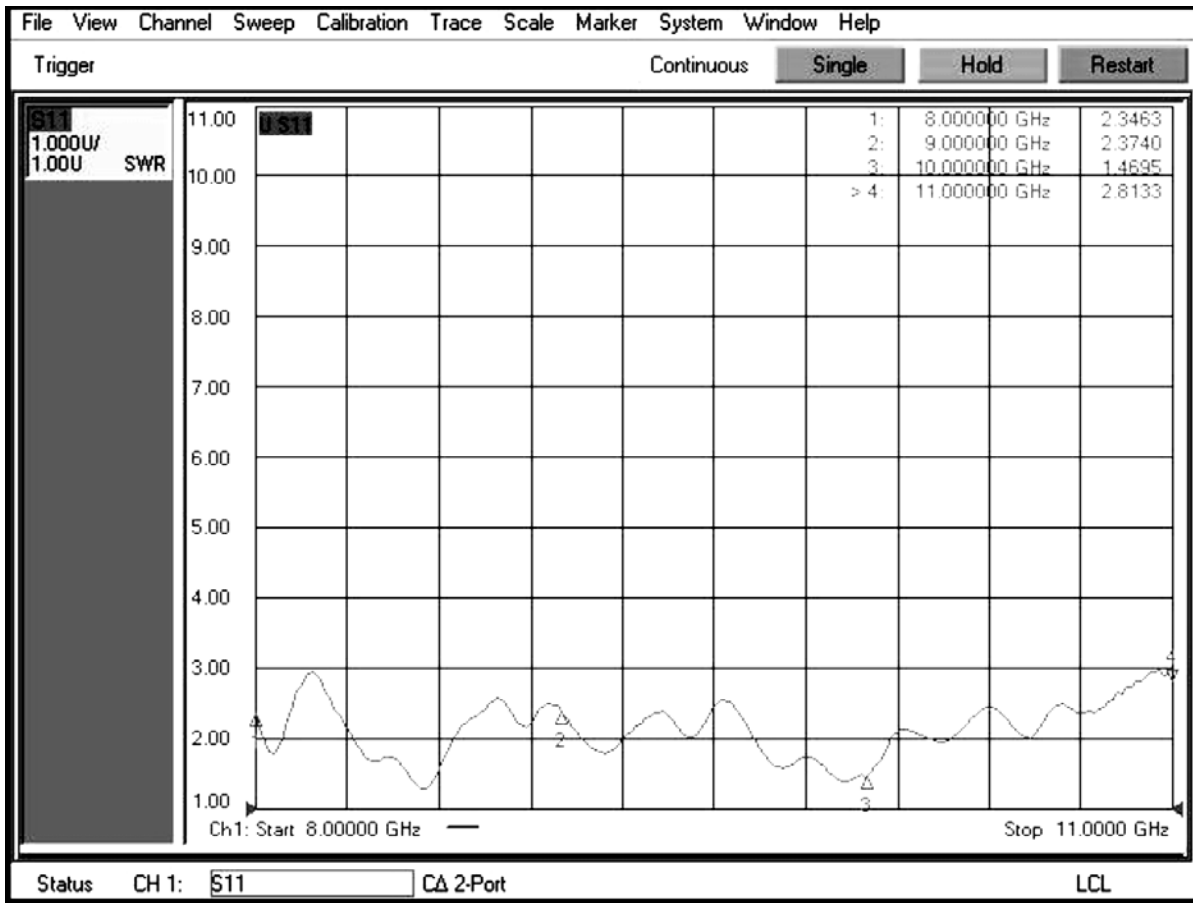


Figure 14: Fabricated Vivaldi array antenna and measurement set up in anechoic chamber

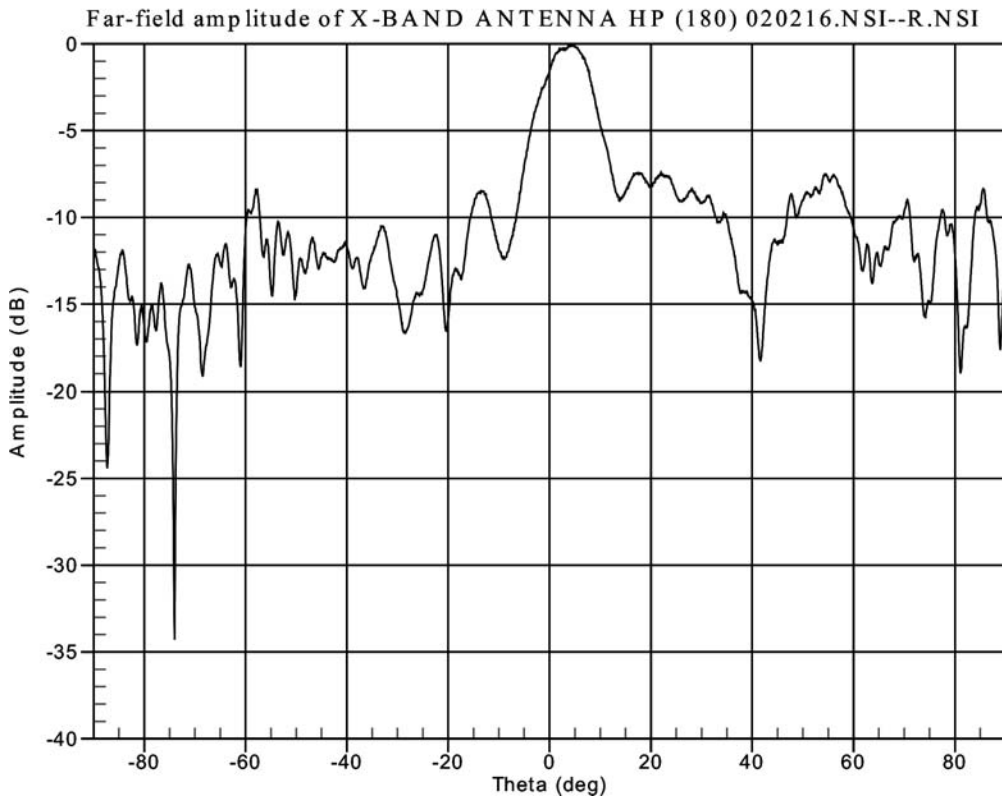


(a) S-parameter

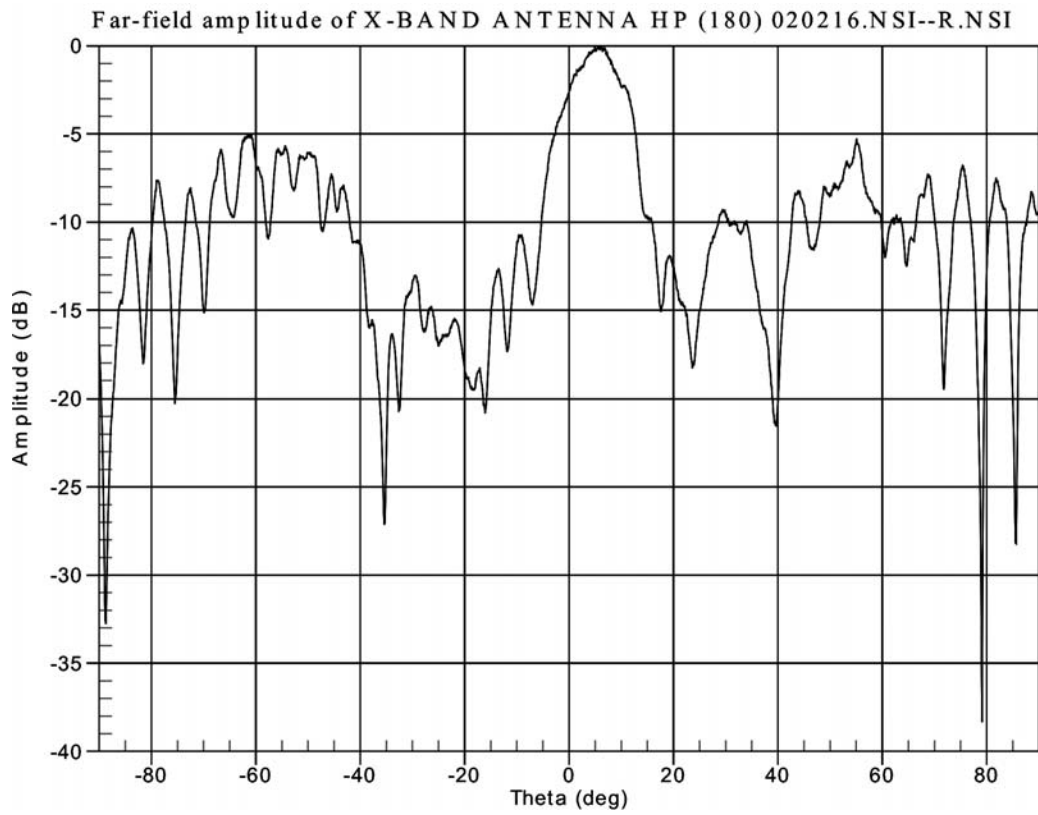


(b) VSWR

Figure 15: Measured S-parameter and VSWR results of 9-elements Vivaldi array antenna



(a) at 9GHz



(b) at 10GHz

Figure 16: Measured Radiation patterns of 9-elements Vivaldi array antenna in H-plane

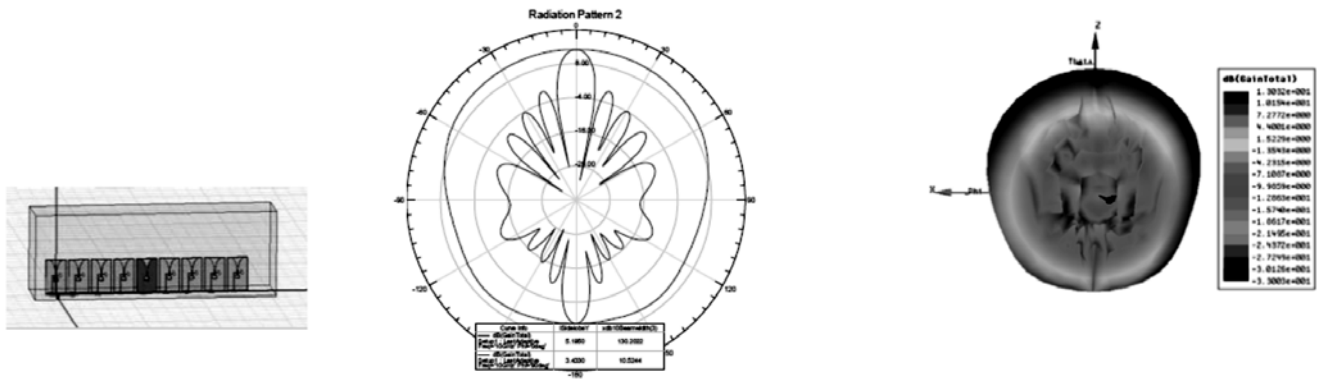


Figure 17: Simulated Radiation patterns of linear array

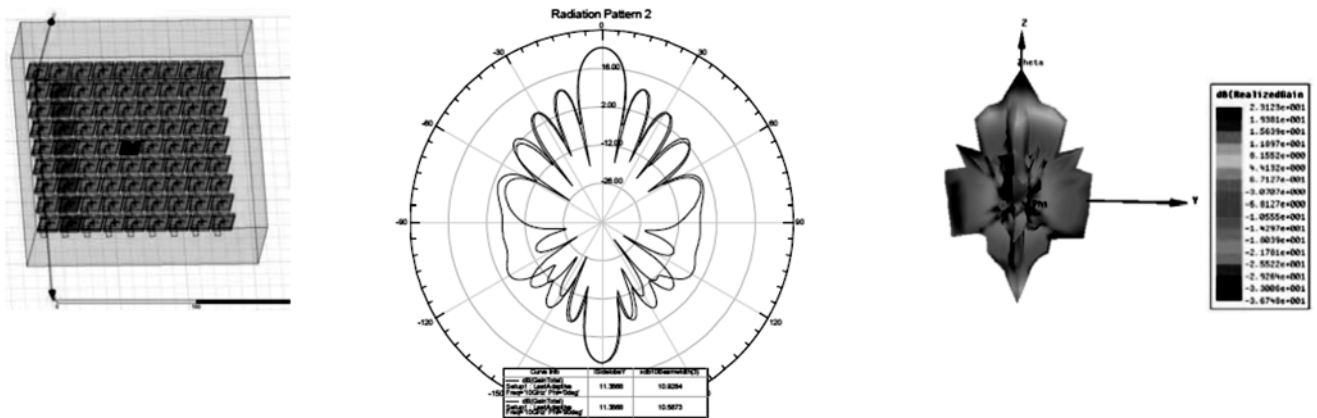


Figure 18: Simulated Radiation patterns of planar array

5. CONCLUSION

This paper started with a tapered slot antenna element design for radar applications. The antenna has a total size equal to $14.2 \times 24.1 \times 1.4$ mm³ and is capable of achieving approximately 10% bandwidth at X-band experimentally. The measured results of single element have shown a widebeam width and a gain of around 4dBi over X-band frequency in array environment. The 9-element array and feeding network based on T-junction power dividers were employed to compose the linear array. The power distribution among the radiating elements is realized using a uniform distribution. The 9-element array was fabricated and measured over X-band frequency. The radiation performances of the array are good for the full scan area $\pm 60^\circ$. The designed antenna element is suitable for X-band airborne active phased array radars in combat aircraft.

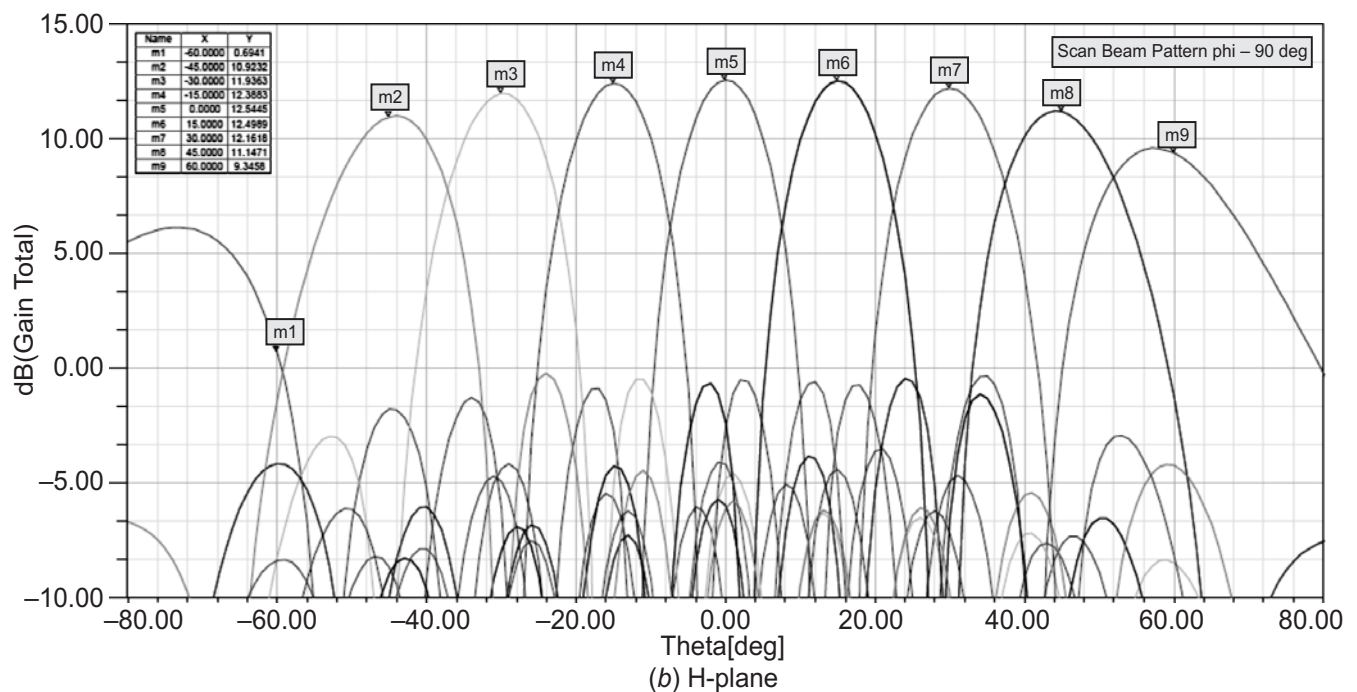
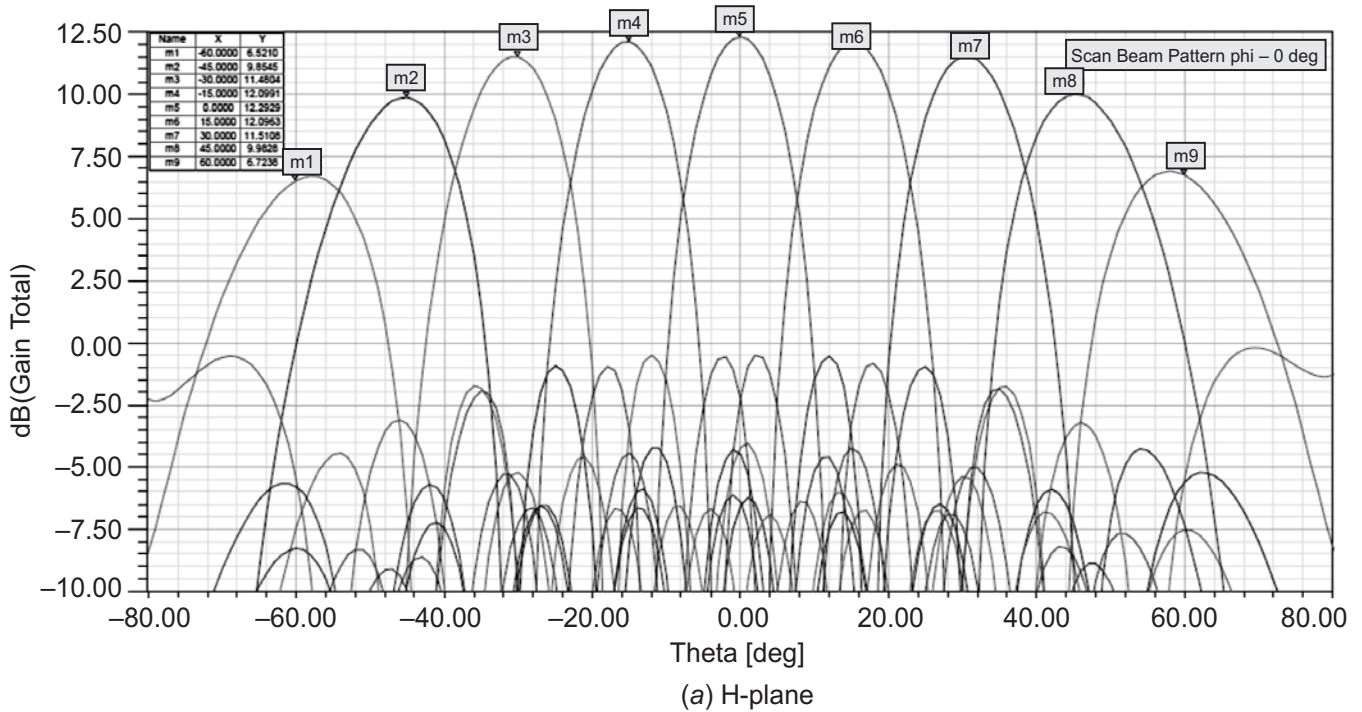


Figure 19: Scanned Multi Beam Patterns of array antenna in both principal planes

6. ACKNOWLEDGMENT

The authors acknowledge the support extended by DRDO in carrying out the work. They equally thank the antenna measurement and fabrication divisions at LRDE for their support in realizing the structure.

7. REFERENCES

1. L.R. Lewis, M. Fasset, and J.Hunt, "A Broadband Stripline Array Element," IEEE International Symposium Antennas Propagation dig., pp. 335-337, 1974.
2. P. J. Gibson, "The Vivaldi Aerial," Proc. 9th European Microwave Conf. Brighton, U.K, pp. 101-105, 1979.
3. J. Shin and D.H. Schaubert, "A Parameter Study of Stripline-Fed Vivaldi Notch Antenna Arrays," IEEE Trans. Antennas Propagation, Vol. 47, pp. 879-886, 1999.
4. Khabat Ebnabbasi, Dan Busuioc, Ralf Birken, and Ming Wang, "Taper Design of Vivaldi and Co-Planar Tapered Slot Antenna (TSA) by Chebyshev Transformer," IEEE Transactions on Antennas and Propagation, vol. 60, no. 5, May 2012.
5. Wormhole attacks in mobile ad hoc networks" at National conference Advances in computer, Information and Applied Science on 11th April 2015 organized by Dept of MCA, Sona college of Technology April 2015.
6. A.M. Abbosh and M.E. Bialkowski, "Compact directional antenna for ultra wideband microwave imaging system," Microwave Optical Tech. letters, Vol. 51, No. 12, pp. 2898-2901, Dec. 2009.
7. S. Ramesh and T.R. Rao, "Dielectric Loaded Exponentially Tapered Slot Antenna for Wireless Communications at 60 GHz," Progress in Electromagnetics Research C, Vol.38, pp. 43-54, 2013.
8. J.H. Shafieha, J. Noorinia and C. Ghobadi, "Probing the feed line parameters in Vivaldi notch antennas," Progress in Electromagnetics Research B, Vol. 1, pp. 237-252, 2008.
9. Challenges and Surveys in Key Management and Authentication Scheme for Wireless Sensor Networks" in Abstract of Emerging Trends in Scientific Research 2014– 2015. <https://ideas.repec.org/s/pkp/abetsr.html> A.K. Bhattacharyya, "Phased Array Antennas," John Wiley and Sons Inc., 2006.
10. H.J. Visser, "Array and Phased Array Antenna Basics", John Wiley and Sons, 2005.
11. Energy Efficient Two-Phase Sensing for Cooperative Spectrum Sensing in Cognitive Radio Ad hoc Networks" in Central government NISCAIR, Journal of Scientific & Industrial Research (JSIR), New Delhi, india in September 2016 issue Bengt Svensson, Jonas Wingard, "A wide scan phased array antenna for a small active electronically scanned array," The Fourth IASTED International Conference on Antennas, Radar and Wave Propagation (ARP), 2007.
12. Chen, M. and J.Wang, "Planar UWB antenna array with CPW feeding network," Proceedings of Asia-Pacific Microwave Conference (APMC), 1-4, 2008.